Supplementary Information for

FimH confers mannose-targeting ability to Bacillus Calmette-Guerin for improved immunotherapy in bladder cancer

Yang Zhang, Fan Huo, Qiang Cao, Ru Jia, Qiju Huang, Zhu A. Wang, Dan Theodorescu, Qiang Lv, Pengchao Li, Chao Yan

Corresponding authors: Qiang Lv, Pengchao Li, Chao Yan (yanchao@nju.edu.cn).

This PDF file includes:

Figures S1 to S7

Zhang Y, *et al. J Immunother Cancer* 2022; 10:e003939. doi: 10.1136/jitc-2021-003939

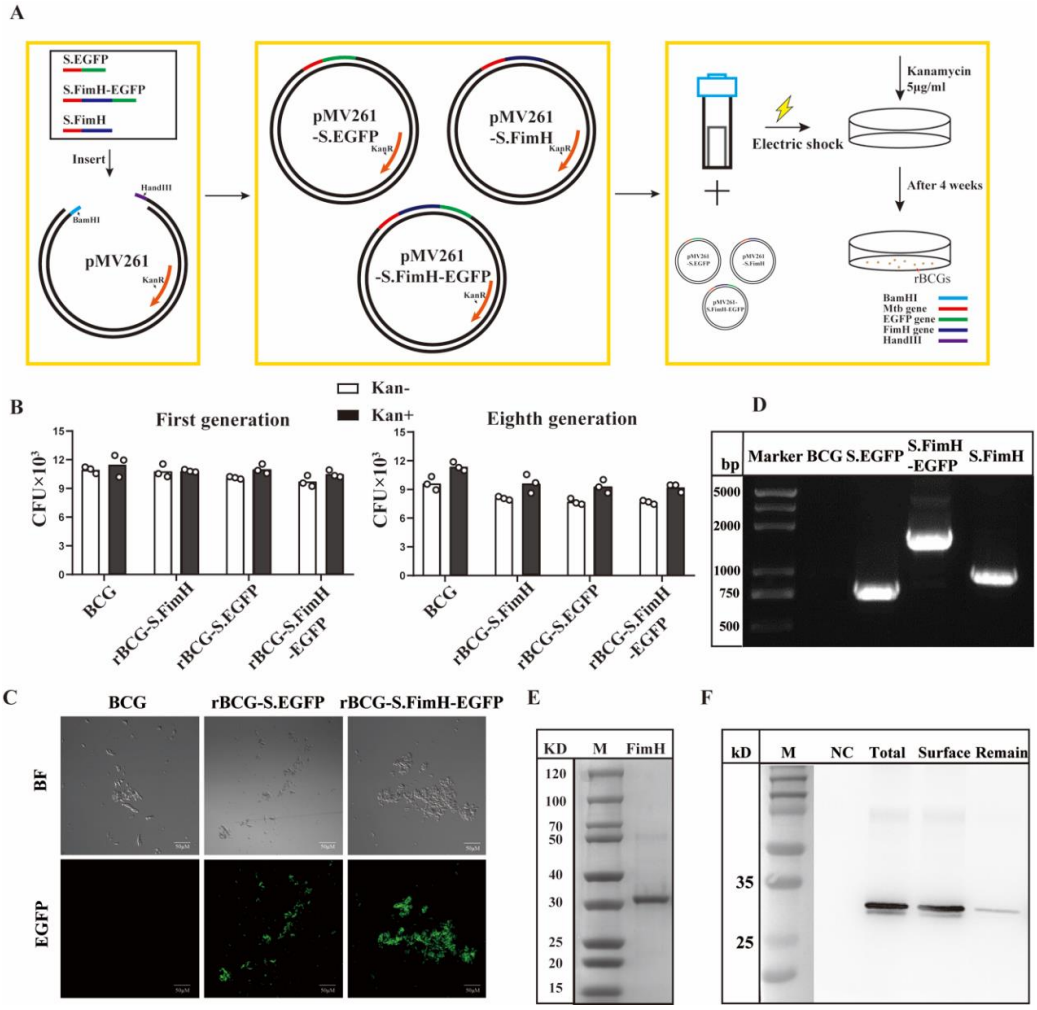

Supplementary Figure S1. Generation and characterization of recombinant BCG overexpressing the FimH protein on the outer surface. (**A**) Schematic representation of the construction process of rBCG.FimH, rBCG-S.EGFP and rBCG-S.FimH-EGFP. (**B**) Stability testing of all recombinant BCG strains. BCG were cultured with or without the kanamycin selection pressure. All the recombinant strains were stable after eight generations even without kanamycin selection. (**C**) Fluorescence microscopy analysis of BCG strains. Positive green fluorescence signal indicated the successful construction of recombinant BCG expressing S.EGFP or S.FimH-EGFP. BF: bright field. Scale bar: 50 μm. (**D**) RT-PCR analysis of FimH mRNA levels in recombinant BCG overexpressing S.EGFP, S.FimH-EGFP or S.FimH. (**E**) pET28a-FimH plasmids were transfected into BL21 and the FimH protein was purified on a nickel column for the generation of rabbit polyclonal antibodies. Shown is the purified FimH separated on SDS-PAGE. (**F**) Immunoblotting result showing the successful expression of FimH protein on the surface of rBCG-S.FimH. NC: BCG.

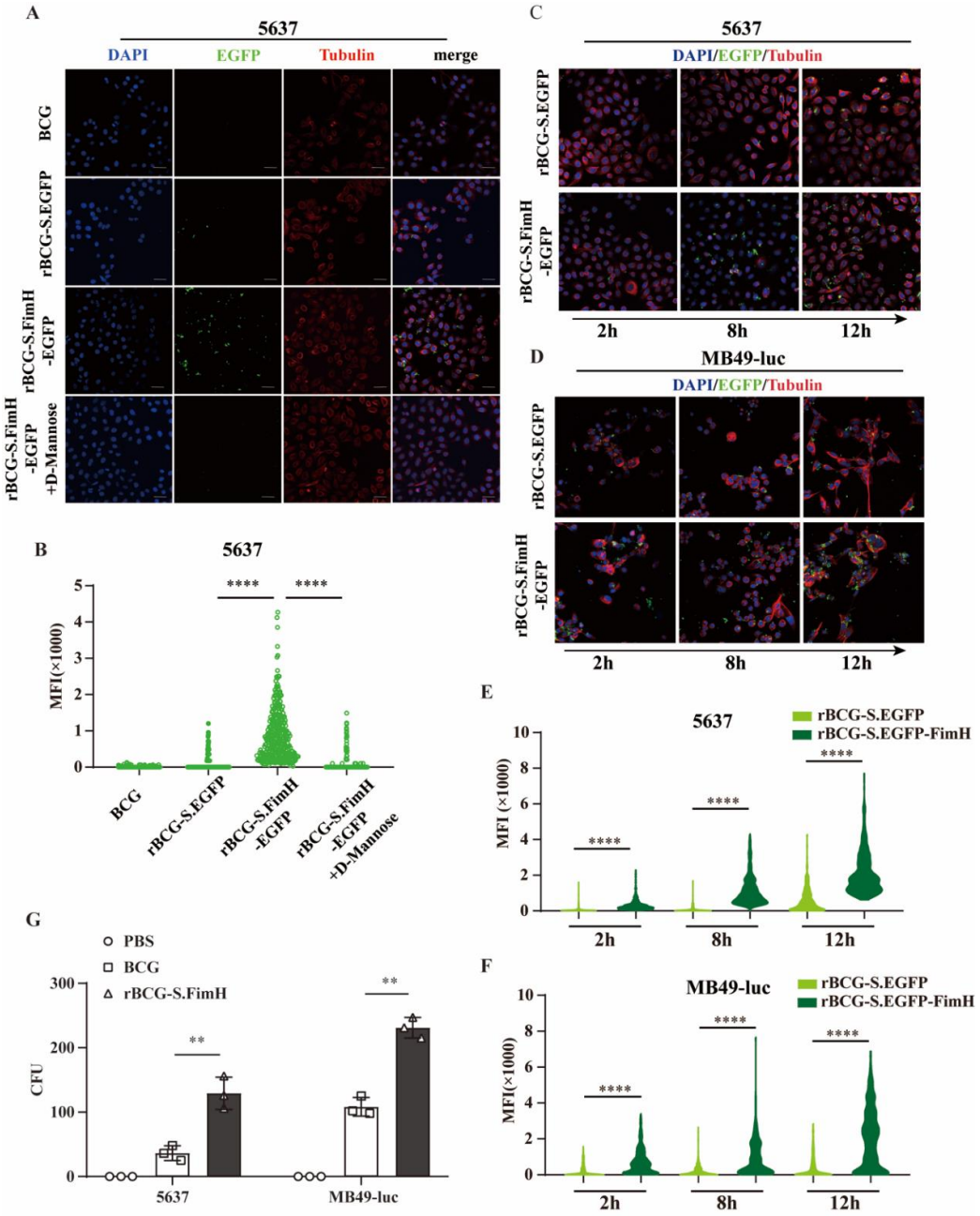

Supplementary Figure S2. rBCG-S.FimH exhibited stronger adhesion and internalization ability *in vitro*. (**A-B**) Human bladder cancer cell line 5637 was incubated with BCG, rBCG-S.EGFP and rBCG-S.FimH-EGFP with or without free D-mannose for 4 h, fluorescence images were taken by confocal (A) and fluorescence intensity quantitated using Image J (B). Scale bar: 50 μm. (**C-F**) Human bladder cancer cell line 5637 (C, E) and mouse bladder cancer cell line MB49-luc (D, F) were incubated with rBCG-S.EGFP

or rBCG-S.FimH-EGFP for 2, 8, 12 hours, respectively, fluorescence images were taken by confocal (C-D) and fluorescence intensity quantitated using Image J (E-F). Scale bar: 50 μm. (**G**) The amount of BCG internalized into 5637 or MB49 cells were analyzed using the colony formation unit (CFU) assay. ** $p<0.01$, **** $p<0.0001$.

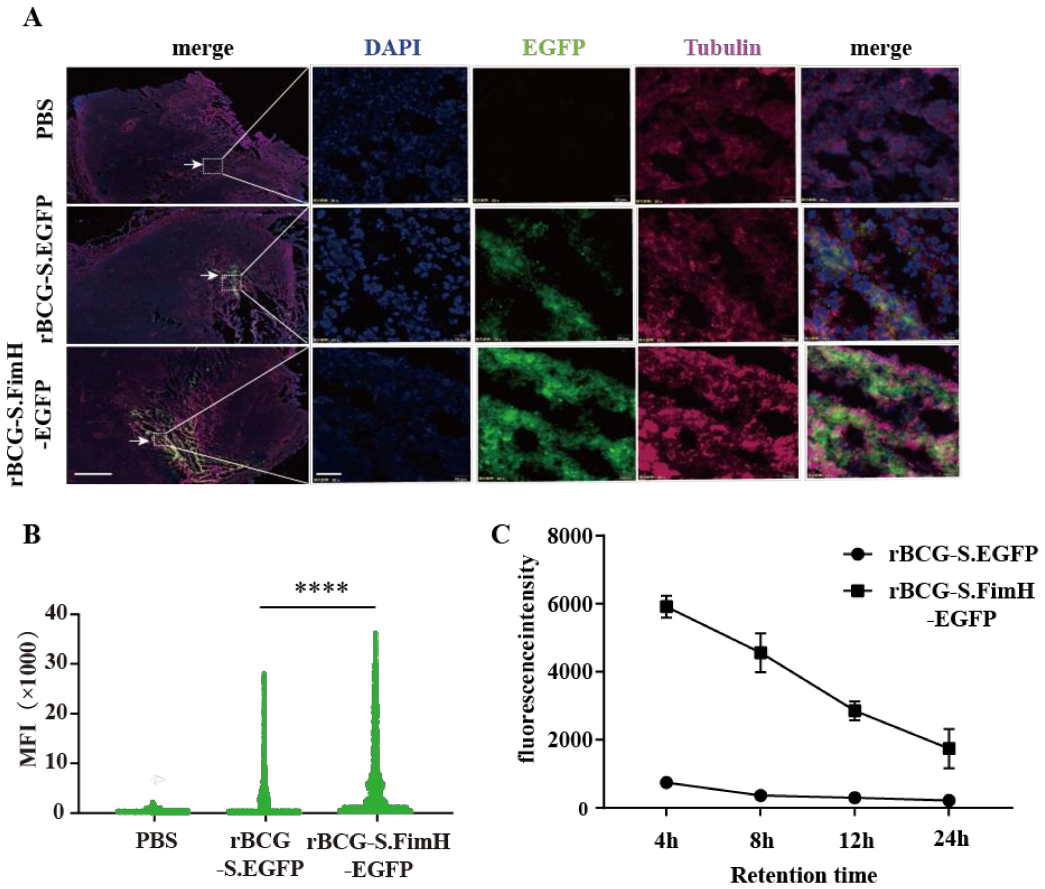

Supplementary Figure S3. rBCG-S.FimH exhibited stronger attachment and longer retention time in orthotopic tumor-bearing mouse bladder. (**A-B**) MB49-luc tumor-bearing mice were deprived of water for 8 hours, followed by intravesical injection with PBS, rBCG-S.EGFP or rBCG-S.FimH-EGFP (5×10^5 CFU/ml, 50 µl/mice), the bladders were collected 4 hours later and frozen sections were subjected to immunofluorescence staining (A) and quantitation using Image J (B). Scale bar: 20 µm. **** $p<0.0001$. (**C**) rBCG-S.FimH-EGFP showed higher retention time in normal mouse bladder compared with rBCG-S.EGFP.

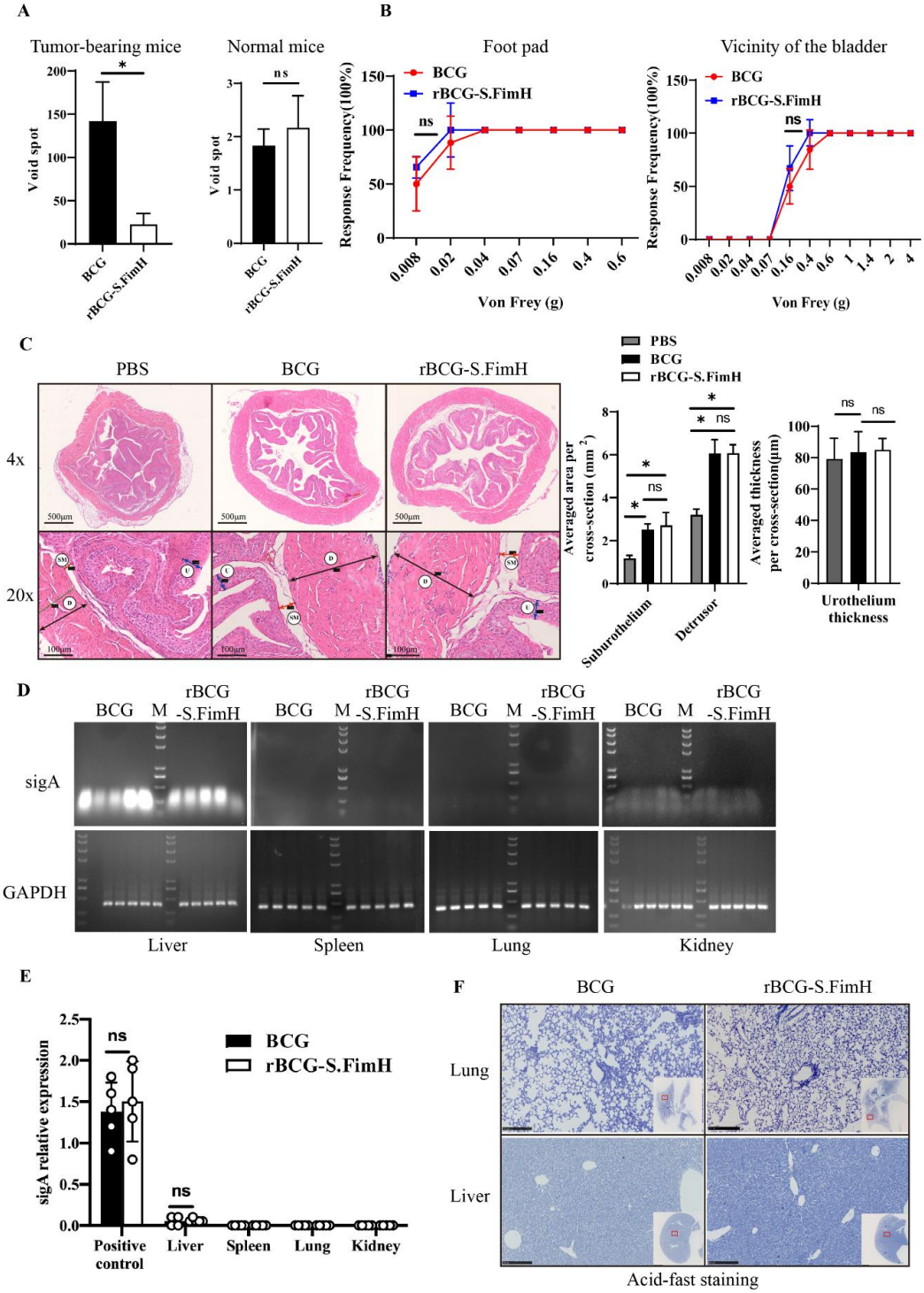

Supplementary Figure S4. rBCG-S.FimH induced similar degree of cystitis and BCGitis in mice. MB49-luc tumor-bearing mice or normal mice that have received a full

course of intravesical treatment with wild-type BCG or rBCG-S.FimH were compared for BCG-induced cystitis and BCGitis. (**A**) The frequency of urination was measured for 4 h using the void spot assay in both tumor-bearing mice and normal mice. (**B**) Pelvic pain in tumor-bearing mice was evaluated using the von Frey test on either the footpad or the abdominal area. (**C**) Histological analysis of the detrusor muscle, the sub-urothelial layer (including submucosa and lamina propria but excluding urothelium) and the urothelium showing similar degree of cystitis in both groups (D, detrusor; LP, lamina propria; SM, submucosa; U, urothelium). (**D-E**) BCG infection of mouse organs including the liver, lung, spleen and kidney was evaluated by PCR analysis of the BCG-specific gene SigA. (**F**) BCG infection of mouse organs was also evaluated using the acid-fast stain method. Scale bar: 100 μm. * $p<0.05$.

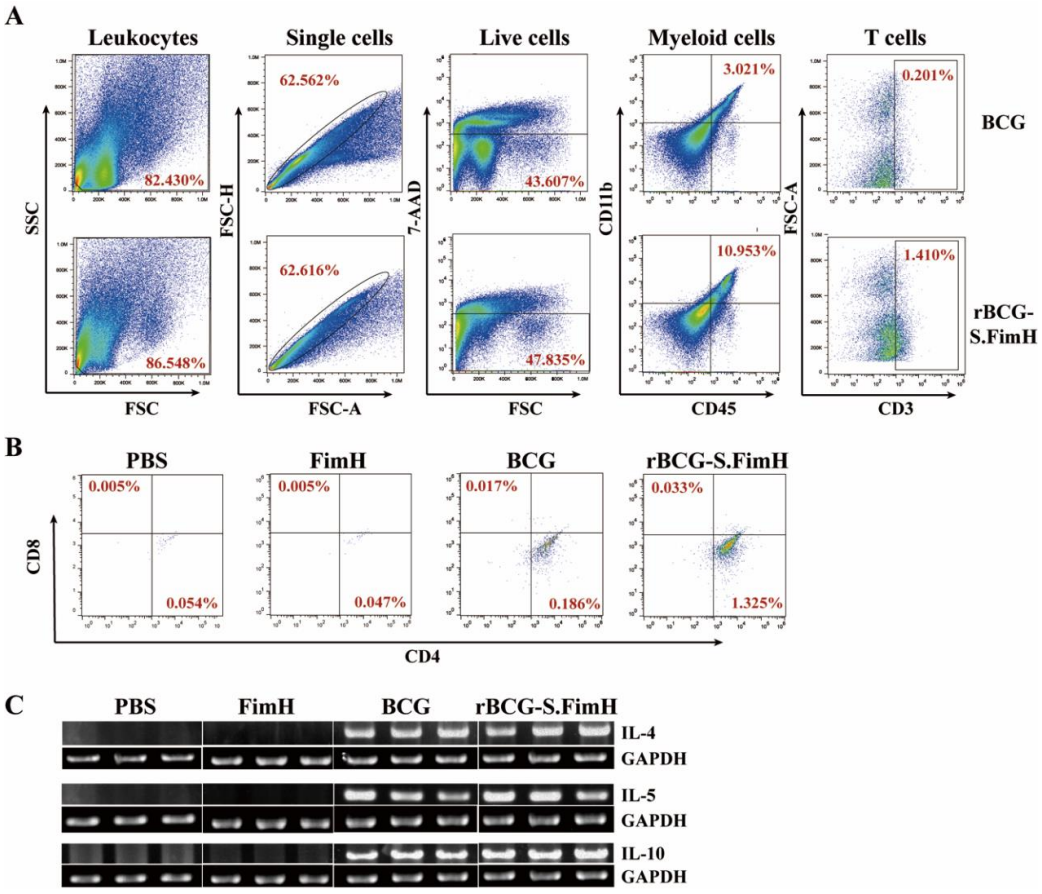

Supplementary Figure S5. Definition of CD4 and CD8-postivie T cells in the bladder. (**A**) The bladders were harvested from MB49-luc tumor-bearing mice and the cells were stained with CD45, CD11b and CD3. CD45+CD11b+CD3+ live leukocytes were defined as T cells. (**B**) The T cells were analyzed for CD4 and CD8 expression. Representative flow data were shown. (**C**) Compared with BCG, rBCG-S.FimH did not enhance Th2 immune response, as represented by IL-4, IL-5, IL-10 mRNA levels in the bladder (n = 3).

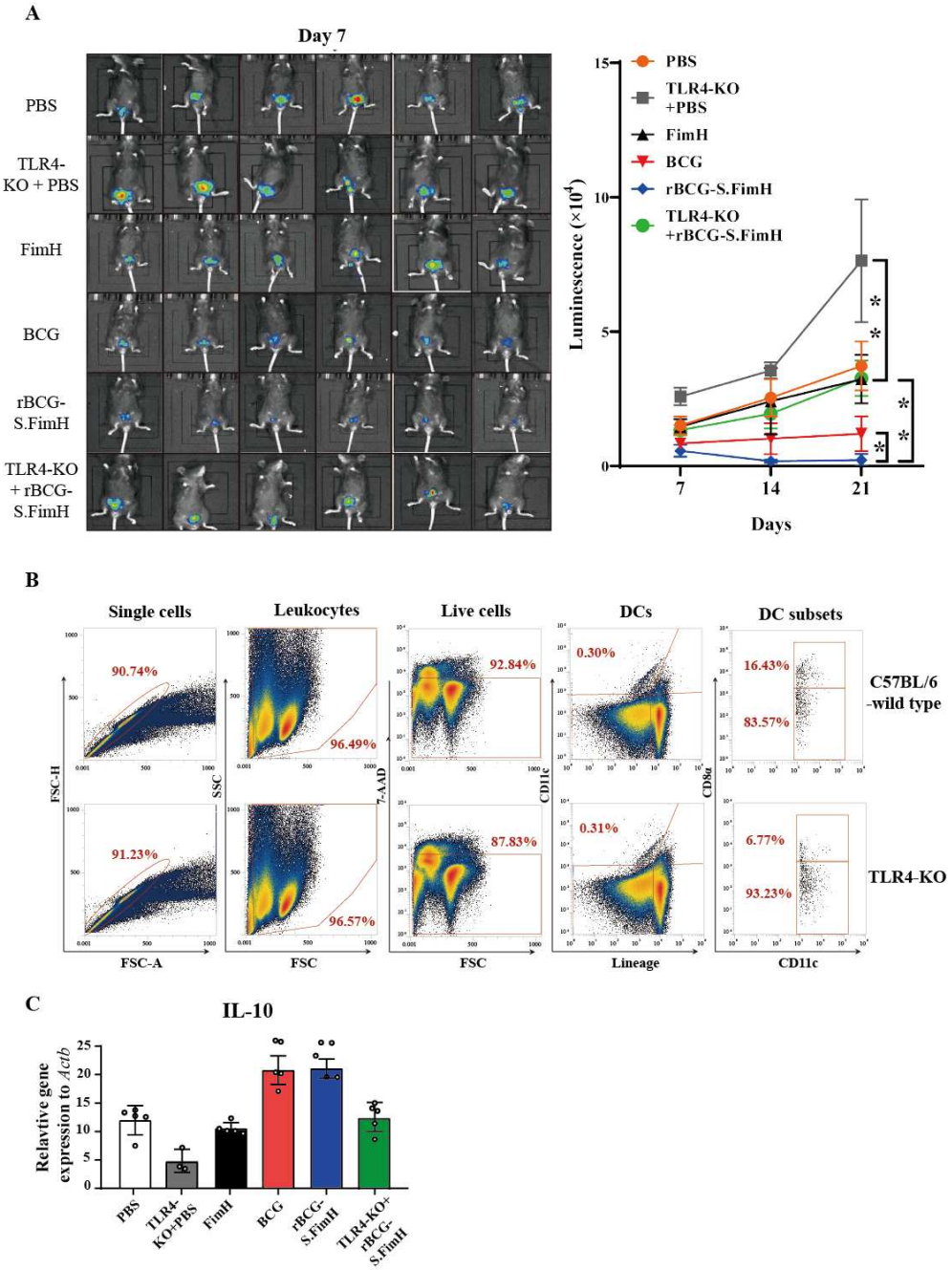

Supplementary Figure S6. rBCG-S.FimH did not promote Th2 immune responses in the inguinal lymph node. (**A-B**) C57BL/6 mice (n = 6 per group) were intravesically inoculated with 1×10^6 MB49-luc cells, and treated with PBS, 2.5 mg/kg of FimH, 2.5×10^5 CFU/ml BCG or rBCG-S.FimH instillation twice a week for 4 weeks. (**A**) IVIS images of mice from different treatment groups at day 7. (**B**) The growth curve of tumors

as monitored by IVIS from day 7 to day 21. (**C**) Definition of dendritic cells (DCs) in the inguinal lymph nodes. iLN was harvested from MB49-luc tumor-bearing mice and the cells were stained with lineage markers and CD11c. The lineage markers included were anti-B220, anti-CD3, anti-CD49b, anti-Gr1, anti-Thy1.1, and anti-TER-119. Lineage-CD11c+ live leukocytes were defined as DCs. The DCs were further divided into CD8α+ and CD8α- subpopulations. (**D**) MB49-luc tumor-bearing C57BL/6 and TLR4-KO mice were intravesically instilled with PBS, 2.5 mg/kg of FimH, 2.5×10^5 CFU/ml BCG or rBCG-S.FimH twice a week for 4 weeks. The iLNs were harvested and mRNA levels of IL-10 analyzed by Q-PCR (data presented as mean ± SD). * $p<0.05$, ** $p<0.01$.

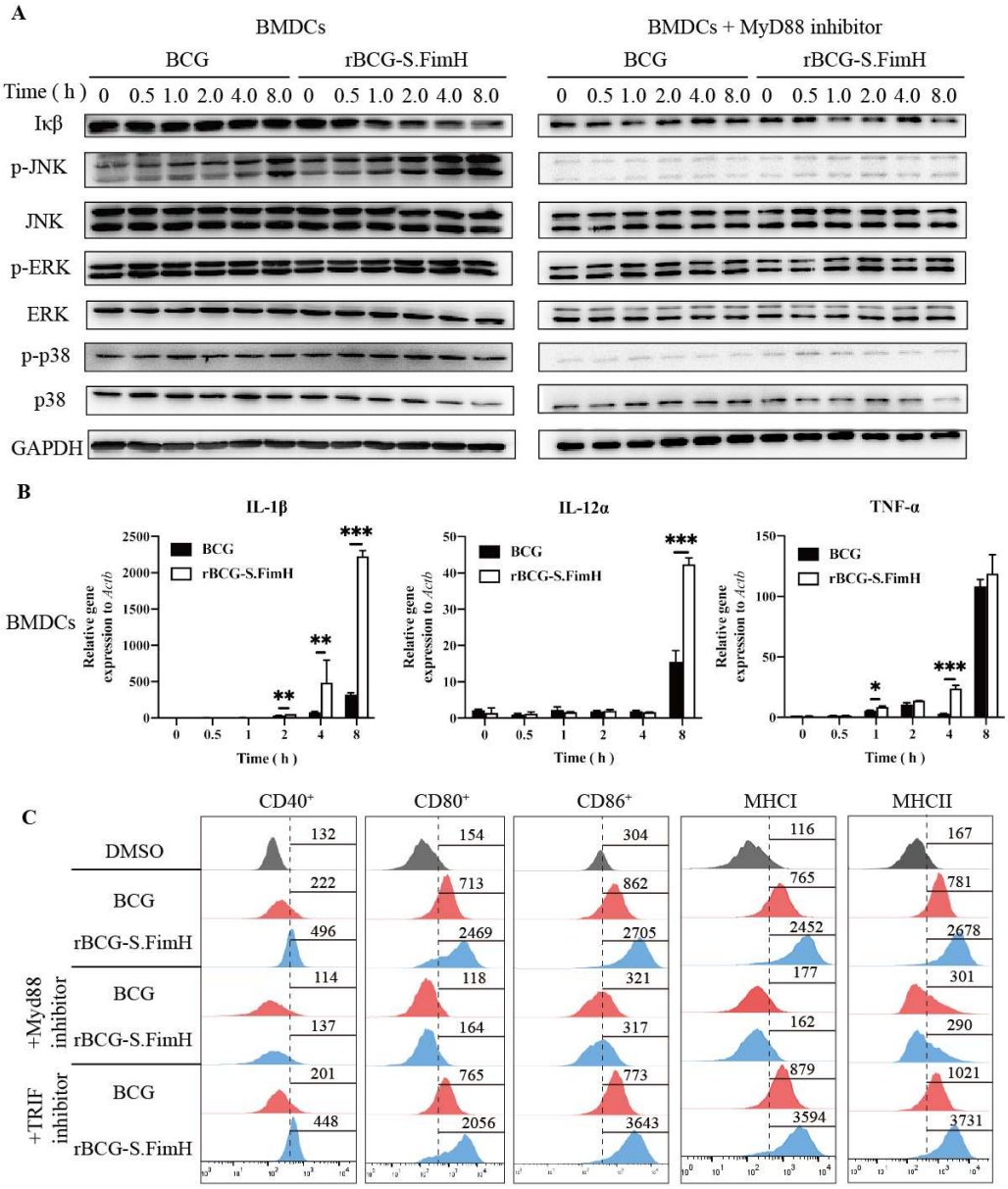

Supplementary Figure S7. rBCG-S.FimH activated the TLR4 pathway in bone marrow-derived DC cells. (**A**) Mouse bone marrow-derived DC (BMDC) cells were treated with wild-type BCG or rBCG-S.FimH in the absence or presence of MyD88 inhibitor for different times, the levels of signaling molecules downstream of TLR4 were determined by western blotting. (**B**) IL-1β, IL12 and TNF-α expression levels in BMDC cells were determined by RT-PCR. (**C**) MyD88 inhibition but not TRIF inhibition significantly blocked rBCG-S.FimH induced upregulation of CD40/CD80/CD86 and MHCI/II expression in BMDC cells. Representative flow cytometry images were shown.